5-Fluorouracil, which is one of the key drugs for treatment of esophageal cancer, was also reported to have immediate cardiotoxicity (20). However, in the present study, concurrent chemotherapy did not significantly enhance the radiation-induced myocardial injury. Although it might not enhance radiation cardiotoxicity in the late phase, the influence of chemotherapy is unclear because chemotherapy is often not performed in patients with poor creatinine clearance.

Although there was no investigation of the relationship between BNP or MMP-3 concentrations and dose–volume of the left ventricle in the present study, Rutqvist *et al.* (21) and Gyenes *et al.* (22) analyzed mortality from ischemic heart disease according to estimated heart dose–volume and found that the cumulative mortality rate was significantly higher in patients in the high dose–volume subgroup than in patients who received no radiotherapy. Thus, radiation oncologists may have to make efforts to reduce irradiated cardiac volume to minimize the risk of radiation-associated adverse events. However, the thoracic esophagus is located close behind the heart and near the lung and spinal cord, which are important critical organs. Recently, there have been some reports of treatment for esophageal cancer using intensity-modulated radiation therapy (23, 24). It is hard to avoid the heart being irradiated to some extent, and it is necessary to establish the constraints of heart.

CONCLUSIONS

In this study, we found that the level of BNP was significantly increased more than 9 months after the start of radiotherapy for the mediastinum and that the levels of BNP and MMP-3 were significantly higher in patients who had high FDG accumulation corresponding to the irradiated field, indicating the need for careful follow-up of such patients. Although the relationships between prognosis and BNP or MMP-3 levels should be investigated further, the results of this study indicate that plasma BNP and MMP-3 concentrations might be early indicators of radiation-induced myocardial damage.

REFERENCES

1. Murakami M, Kuroda Y, Nakajima T, *et al.* Comparison between chemoradiation protocol intended for organ preservation and conventional surgery for clinical T1-T2 esophageal carcinoma. *Int J Radiat Oncol Biol Phys* 1999;45:277–284.
2. Hironaka S, Ohtsu A, Boku N, *et al.* Nonrandomized comparison between definitive chemoradiotherapy and radical surgery in patients with T(2-3)N(any) M(0) squamous cell carcinoma of the esophagus. *Int J Radiat Oncol Biol Phys* 2003;57: 425–433.
3. Yamada S, Nemoto K, Takai Y, *et al.* Proposal for standard radiotherapy methods for superficial esophageal cancer. A multicenter retrospective evaluation. *J JASTRO* 2000;12:169–176.
4. Jingu K, Nemoto K, Kaneta T, *et al.* A case of high FDG-uptake into the myocardium after radiotherapy for esophageal cancer. *Nippon Igaku Hoshasen Gakkai Zasshi* 2005;65:266–269.
5. Jingu K, Kaneta T, Nemoto K, *et al.* The utility of ^{18}F-fluorodeoxyglucose positron emission tomography for early diagnosis of radiation-induced myocardial damage. *Int J Radiat Oncol Biol Phys* 2006;66:845–851.
6. Saito Y, Nakao K, Yamada T, *et al.* Brain natriuretic peptide is a novel cardiac hormone. *Biochem Biophys Res Commun* 1989; 158:360–368.
7. Kambayashi Y, Nakao K, Mukoyama M, *et al.* Isolation and sequence determination of human brain natriuretic peptide in human atrium. *FEBS Lett* 1990;259:341–345.
8. Mukoyama M, Nakao K, Hosoda K, *et al.* Brain natriuretic peptide as a novel cardiac hormone in humans. Evidence for an exquisite dual natriuretic peptide system, atrial natriuretic peptide and brain natriuretic peptide. *J Clin Invest* 1991;87:1402–1412.
9. Levin ER, Gardner DG, Samson WK. Natriuretic peptides. *N Engl J Med* 1998;339:321–328.
10. Dollery CM, McEwan JR, Henney AM. Matrix metalloproteinases and cardiovascular disease. *Circ Res* 1995;77:863–868.
11. Galis ZS, Muszynski M, Sukhova GK, *et al.* Cytokine stimulated human vascular smooth muscle cells synthesize a complement of enzymes required for extracellular matrix digestion. *Circ Res* 1994;75:181–189.
12. Nagase H, Okada Y. Proteinases and matrix degradation. In: Kelly WN, Harris ED, Ruddy S, *et al.*, editors. Textbook of rheumatology. New York: W.B. Saunders; 1997. p. 323–341.
13. Spinale FG, Coker ML, Bond BR, *et al.* Myocardial matrix degradation and metalloproteinase activation in the failing heart: A potential therapeutic target. *Cardiovasc Res* 2000;46:225–238.
14. Wondergem J, Persons K, Zurcher C, *et al.* Changes in circulating atrial natriuretic peptide in relation to the cardiac status of Rhesus monkeys after total-body irradiation. *Radiother Oncol* 1999;53:67–75.
15. Wondergem J, Strootman EG, Frolich M, *et al.* Circulating atrial natriuretic peptide plasma levels as a marker for cardiac damage after radiotherapy. *Radiother Oncol* 2001;58:295–301.
16. Kruse JJ, Strootman EG, Bart CI, *et al.* Radiation-induced changes in gene expression and distribution of atrial natriuretic peptide (ANP) in different anatomical regions of the rat heart. *Int J Radiat Biol* 2002;78:297–304.
17. Meinardi MT, van Veldhuisen DJ, Gietema JA, *et al.* Prospective evaluation of early cardiac damage induced by epirubicin-containing adjuvant chemotherapy and locoregional radiotherapy in breast cancer patients. *J Clin Oncol* 2001;15:2746–2753.
18. Cowie MR, Struthers AD, Wood DA, *et al.* Value of natriuretic peptides in assessment of patients with possible new heart failure in primary care. *Lancet* 1997;350:1349–1353.
19. Maisel AS, Krishnaswamy P, Nowak RM, *et al.* Rapid measurement of B-type natriuretic peptide in the emergency diagnosis of heart failure. *N Engl J Med* 2002;347:161–167.
20. Schimmel KJ, Richel DJ, van den Brink RB, *et al.* Cardiotoxicity of cytotoxic drugs. *Cancer Treat Rev* 2004;30:181–191.
21. Rutqvist LE, Lax I, Fornander T, *et al.* Cardiovascular mortality in a randomized trial of adjuvant radiation therapy versus surgery alone in primary breast cancer. *Int J Radiat Oncol Biol Phys* 1992;22:887–896.
22. Gyenes G, Rutqvist LE, Liedberg A, *et al.* Long-term cardiac morbidity and mortality in a randomized trial of pre- and postoperative radiation therapy versus surgery alone in primary breast cancer. *Radiother Oncol* 1998;48:185–190.
23. Chandra A, Guerrero TM, Liu HH, *et al.* Feasibility of using intensity-modulated radiotherapy to improve lung sparing in treatment planning for distal esophageal cancer. *Radiother Oncol* 2005;77:247–253.
24. Wu VW, Sham JS, Kwong DL. Inverse planning in three-dimensional conformal and intensity-modulated radiotherapy of mid-thoracic oesophageal cancer. *Br J Radiol* 2004;77: 568–572.

Hypofractionated Stereotactic Radiotherapy (HypoFXSRT) for Stage I Non-small Cell Lung Cancer: Updated Results of 257 Patients in a Japanese Multi-institutional Study

Hiroshi Onishi, MD, Hiroki Shirato, MD,† Yasushi Nagata, MD,† Masahiro Hiraoka, MD,‡ Masaharu Fujino, MD,† Kotaro Gomi, MD,§ Yuzuru Niibe, MD,|| Katsuyuki Karasawa, MD,|| Kazushige Hayakawa, MD,¶ Yoshihiro Takai, MD,# Tomoki Kimura, MD,** Atsuya Takeda, MD,†† Atsushi Ouchi, MD,‡‡ Masato Hareyama, MD,‡‡ Masaki Kokubo, MD,§§ Ryusuke Hara, MD,|||| Jun Itami, MD,|||| Kazunari Yamada, MD,¶¶ and Tsutomu Araki, MD**

Introduction: Hypofractionated stereotactic radiotherapy (HypoFXSRT) has recently been used for the treatment of small lung tumors. We retrospectively analyzed the treatment outcome of HypoFXSRT for stage I non-small cell lung cancer (NSCLC) treated in a Japanese multi-institutional study.

Methods: This is a retrospective study to review 257 patients with stage I NSCLC (median age, 74 years: 164 T1N0M0, 93 T2N0M0) were treated with HypoFXSRT alone at 14 institutions. Stereotactic three-dimensional treatment was performed using noncoplanar dynamic arcs or multiple static ports. A total dose of 18 to 75 Gy at the isocenter was administered in one to 22 fractions. The median calculated biological effective dose (BED) was 111 Gy (range, 57–180 Gy) based on $\alpha/\beta = 10$.

Results: During follow-up (median, 38 months), pulmonary complications of above grade 2 arose in 14 patients (5.4%). Local progression occurred in 36 patients (14.0%), and the local recurrence rate was 8.4% for a BED of 100 Gy or more compared with 42.9% for less than 100 Gy ($p < 0.001$). The 5-year overall survival rate of medically operable patients was 70.8% among those treated with a BED of 100 Gy or more compared with 30.2% among those treated with less than 100 Gy ($p < 0.05$).

Conclusions: Although this is a retrospective study, HypoFXSRT with a BED of less than 180 Gy was almost safe for stage I NSCLC, and the local control and overall survival rates in 5 years with a BED of 100 Gy or more were superior to the reported results for conventional radiotherapy. For all treatment methods and schedules, the local control and survival rates were better with a BED of 100 Gy or more compared with less than 100 Gy. HypoFXSRT is feasible for curative treatment of patients with stage I NSCLC.

Key Words: Stereotactic radiotherapy, Non-small cell lung cancer, Stage I, Hypofractionated.

(*J Thorac Oncol.* 2007;2: Suppl 3, S94–S100)

*Department of Radiology, School of Medicine, Yamanashi University, Yamanashi, Japan; †Department of Radiology, School of Medicine, Hokkaido University, Sapporo, Japan; ‡Department of Therapeutic Radiology and Oncology, Kyoto University Graduate School of Medicine, Kyoto, Japan; §Department of Radiation Oncology, Cancer Institute Hospital, Tokyo, Japan; ||Department of Radiation Oncology, Tokyo Metropolitan Komagome Hospital, Tokyo, Japan; ¶Department of Radiology, Kitasato University, Kanagawa, Japan; #Department of Radiology, School of Medicine, Tohoku University, Sendai, Japan; **Department of Radiology, School of Medicine, Hiroshima University, Hiroshima, Japan; ††Department of Radiology, Tokyo Metropolitan Hiroo Hospital, Tokyo, Japan; ‡‡Department of Radiology, Sapporo Medical University, Sapporo, Japan; §§Department of Image-Based Medicine, Institute of Biomedical Research and Innovation, Kobe, Japan; ||||Department of Radiation Oncology, International Medical Center of Japan, Tokyo, Japan; ¶¶Department of Radiation Oncology, Tenri Hospital, Tenri, Japan.

Disclosure: The authors report no conflict of interest.

This study was presented in part at the 42nd Annual Meeting of the American Society of Oncology (ASCO), June 2–6, 2006, Atlanta, GA.

Address for correspondence: Hiroshi Onishi, Department of Radiology, School of Medicine, Yamanashi Medical University, 1110 Shimokato, Chuo-city, Yamanashi, Japan 409-3898. E-mail: honishi@yamanashi.ac.jp

ISSN: 1556-0864/07/0207-0094

In Japan, due to the routine use of computed tomography (CT), detection of early-stage lung cancer is increasing. For patients with stage I (T1 or 2, N0, M0) non-small cell lung cancer (NSCLC), full lobar or greater surgical resection and regional lymphadenectomy is the standard treatment choice; the local control rates exceed 80% and the overall 5-year survival rates surpass 50%.[1] However, surgical resection is often not feasible or involves a high risk for lung cancer patients with tobacco-related pulmonary illnesses, severe cardiovascular disease, or other medical conditions. Moreover, a small proportion of the patients who are fit for surgery may refuse it for personal reasons.

Radiotherapy (RT) can offer a therapeutic alternative in these cases, but the outcome with conventional RT is unsatisfactory.[2] The reason for the poor survival with conventional RT is thought to be that the dose of conventional RT is too low to control the local tumor. To give a higher dose to the tumor without increasing the adverse effects, hypofractionated high-dose stereotactic RT (HypoFXSRT) has recently been used to treat small cell lung tumors, particularly in Japan.[3–6] Although the optimal treatment technique and

schedule of HypoFXSRT for stage I NSCLC are unknown, the nationwide number of Japanese patients with stage I NSCLC who are treated with small-volume stereotactic RT (SRT) has increased rapidly.

Therefore, it is meaningful to investigate the results of SRT for stage I NSCLC from many institutions, even in a retrospective manner, despite the large differences in treatment protocols. Previously, we reported the result of a Japanese multi-institutional review of 300 patients with stage I NSCLC treated with SRT.[7] We concluded that SRT with a biological effective dose (BED) of less than 150 Gy is effective for the curative treatment of patients with stage I NSCLC and that the local control and survival rates are better with a BED of 100 Gy or more compared with less than 100 Gy.

The survival rates in selected medically operable patients with a BED of 100 Gy or more were promising and potentially comparable with those of surgery. These results for SRT were encouraging for stage I NSCLC patients; however, the 300 subjects in that report included 17 patients irradiated with comparatively small fractions (<4 Gy) and 26 patients irradiated in combination with conventional RT. This article presents the results for patients irradiated with HypoFXSRT alone in a multi-institutional study. In this study, we compared the reported results for surgery and conventional RT with those for HypoFXSRT.

PATIENTS AND METHODS

Eligibility Criteria

This was a retrospective study to review patients who were treated by HypoFXSRT for their stage I NSCLC in 14 different hospitals in Japan.

All the patients enrolled in this study satisfied the following eligibility criteria: identification of T1N0M0 or T2N0M0 primary lung cancer on chest and abdominal CT, bronchoscopy, bone scintigraphy, or brain magnetic resonance imaging; histological confirmation of NSCLC; performance status of 2 or less according to the World Health Organization (WHO) guidelines; and an inoperable tumor due to a poor medical condition or refusal to undergo surgery.

No restrictions were imposed concerning the locations of eligible tumors, irrespective of whether they were located adjacent to a major bronchus, blood vessel, chest wall, or the esophagus. Patients were informed of the concept, methodology, and rationale of this treatment, which was performed in accordance with the 1983 revision of the Declaration of Helsinki.

Patient Characteristics

The patient pretreatment characteristics are summarized in Table 1. From April 1995 to March 2004, a total of 257 patients with primary NSCLC was treated using high-dose HypoFXSRT in the following 14 institutions: Hokkaido University, Kyoto University, Cancer Institute Hospital, Tokyo Metropolitan Komagome Hospital, Kitasato University, Tohoku University, Hiroshima University, Tokyo Metropolitan Hiroo Hospital, Sapporo Medical University, Institute of Biomedical Research and Innovation, International Medical Center of Japan, Tenri Hospital, Kitami Red Cross Hospital, and University of Yamanashi. Of the 257 patients, 158 were considered medically inoperable mainly because of chronic pulmonary disease, advanced age, or other chronic illness. The remaining 99 patients were considered medically operable, but had refused surgery or had been advised to select HypoFXSRT by medical oncologists.

TABLE 1. Patient Pretreatment Characteristics

Total cases: 257
Age: 39–92 yr (median, 74)
Performance status: PS 0, 109; PS 1, 103; PS 2, 39; PS 3, 6
Pulmonary chronic disease: 168 positive, 89 negative
Histology: 111 squamous cell, 120 adenocarcinoma, 26 other
Stage: 164 IA, 93 IB
Tumor diameter: 7–58 mm (median, 28)
Medical operability: 158 inoperable, 99 operable

Treatment Methods

All the patients were irradiated using stereotactic techniques. For the purposes of this study, all the hypofractionated stereotactic techniques met five requirements: reproducibility of the isocenter of 5 mm or less, as confirmed for every fraction; slice thickness on CT of 3 mm or less for three-dimensional (3-D) treatment planning; irradiation with multiple noncoplanar static ports or dynamic arcs; dose per fraction size more than 4 Gy; and a total treatment period of fewer than 25 days. Details of the techniques and instruments used to achieve SRT in the 14 institutions were summarized in a previous report.[7] The clinical target volume (CTV) marginally exceeded the gross target volume (GTV) by 0 to 5 mm. The planning target volume (PTV) comprised the CTV, a 2- to 5-mm internal margin and a 0–5-mm safety margin. A high dose was concentrated on the tumor-bearing area, while sparing the surrounding normal lung tissues using SRT. The irradiation schedules also differed among the institutions. The number of fractions ranged between 1 and 14, with single doses of 4.4 to 35 Gy. A total dose of 30 to 84 Gy at the isocenter was administered with 6- or 4-MV x-rays within 20% heterogeneity in the PTV dose. No chemotherapy was administered before or during RT.

To compare the effects of various treatment protocols with different fraction sizes and total doses, the BED was used in a linear-quadratic model.[8] Here, the BED was defined as $nd(1 + d/\alpha/\beta)$, with gray units, where n is the fractionation number, d is the daily dose, and α/β is assumed to be 10 for tumors. The BED was not corrected with values for the tumor doubling time or treatment term. In this study, the BED was calculated at the isocenter. The median BED was 111.0 Gy (range, 57.6–180.0). The BED was 100 Gy or more in 215 patients and less than 100 Gy in 42 patients. The median BED for the less than 100 Gy and 100 Gy or more subgroups was 79.6 Gy (range, 57.6–98.6) and 117.0 Gy (range, 100.0–180.0), respectively.

Dose constraints were set for the spinal cord only. The BED limit for the spinal cord was 80 Gy (α/β was assumed to be 2 Gy for chronic spinal cord toxicity).

Evaluation

The objectives of this study were to retrospectively evaluate the toxicity, local control rate, and survival rate according to the BED. All patients underwent follow-up examinations by radiation oncologists. The first examination took place 4 weeks after treatment, and patients were subsequently seen every 1 to 3 months. Tumor response was evaluated using the Response Evaluation Criteria in Solid Tumors by CT.[9] Chest CT (slice thickness, 2–5 mm) was usually obtained every 3 months for the first year and repeated every 4 to 6 months thereafter. A complete response (CR) indicated that the tumor had disappeared completely or was replaced by fibrotic tissue. A partial response (PR) was defined as a 30% or more reduction in the maximum cross-sectional diameter. It was difficult to distinguish between residual tumor tissue and radiation fibrosis. Any suspicious confusing residual density after RT was considered evidence of a PR, so the actual CR rate might have been higher than that given here. Local recurrence was considered to have taken place only when enlargement of the local tumor continued for more than 6 months on follow-up CT. Two radiation oncologists interpreted the CT findings. The absence of local recurrence was defined as locally controlled disease. Lung, esophagus, bone marrow, and skin were evaluated using version 2 of the National Cancer Institute–Common Toxicity Criteria (NCI-CTC).

Statistical Analysis

The local recurrence rates in the two groups were compared with the χ^2 test. The BED among patient groups at each pulmonary toxicity grade was compared using the Kruskal-Wallis test. The cumulative local control and survival curves were calculated and drawn applying the Kaplan-Meier algorithms with day of treatment as the starting point. Subgroups were compared using log-rank statistics. Values of $p < 0.05$ were considered statistically significant. Statistical calculations were conducted using version 5.0 StatView software (SAS Institute, Cary, NC).

RESULTS

All the patients completed the treatment with no particular complaints. The median duration of follow-up for all patients was 38 months (range, 2–128).

Local Tumor Response

Of the 257 patients evaluated using CT, CR was achieved in 66 (25.7%) and PR in 157 (61.1%). The overall response rate (CR + PR) was 86.8%. The overall response rates for tumors with a BED of 100 Gy or more ($n = 215$) or less than 100 Gy ($n = 42$) were 87.5% and 86.7% in 3 years (?), respectively. A typical case of a T1 tumor after HypoFXSRT is shown in Figure 1.

Toxicity

Symptomatic radiation-induced pulmonary complications (NCI-CTC criteria grade >1) were noted in 28 patients (10.9%). Pulmonary fibrosis or emphysema before treatment was observed in 25 (89%) of the 28 patients with pulmonary complications above grade 1. Pulmonary complications of NCI-CTC criteria above grade 2 were noted in only 14

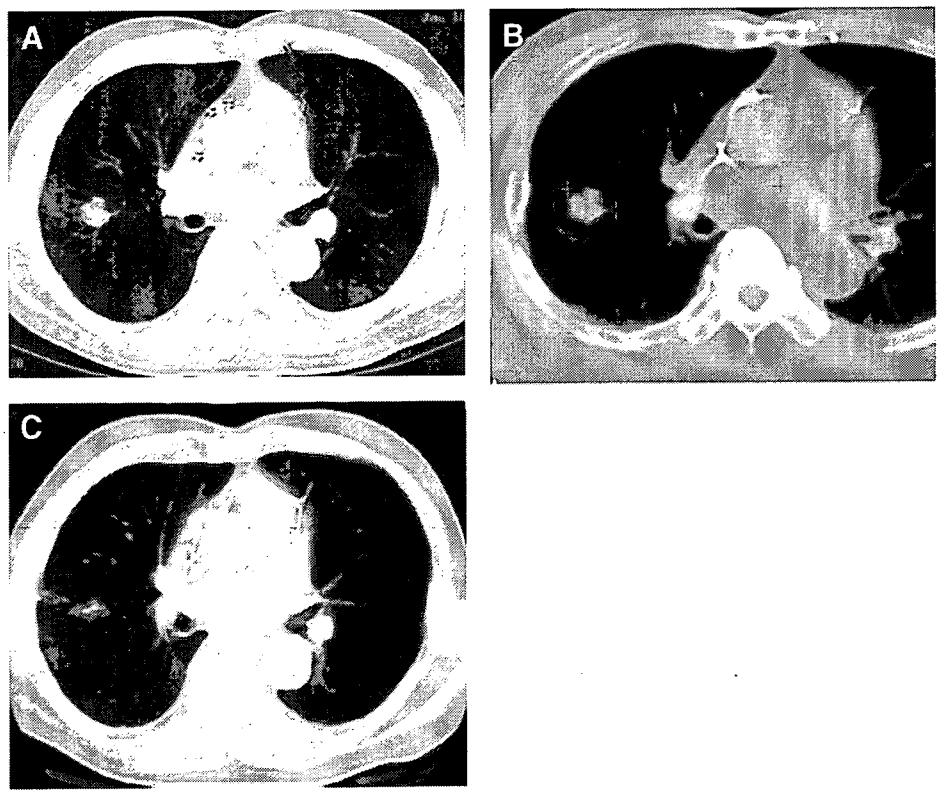

FIGURE 1. A typical example involving SRT for a 76-year-old man with T1N0 adenocarcinoma. He was treated with HypoFXSRT. (*A*) Before hypofractionated stereotactic radiotherapy (HypoFXSRT). (*B*) The calculated dose distribution. The isocenter dose was 75 Gy/10 fractions/5 days, and the tumor was fully enclosed with the 90% dose line. (C) Twelve months after HypoFXSRT, a scarred tumor is rated as a partial response.

TABLE 2. Recurrence Rate According to the BED and Stage

	Total cases	BED <100 Gy	BED ≥100 Gy	*p*	Stage IA	Stage IB	*p*
Local tumor	36/257 (14.0%)	18/42 (42.9%)	18/215 (8.4%)	<0.01	20/164 (12.2%)	16/93 (17.2%)	0.21
Regional nodal metastasis	29/257 (11.3%)	9/42 (21.4%)	20/215 (9.3%)	<0.05	17/164 (10.4%)	12/93 (12.9%)	0.54
Distant metastasis	51/257 (19.8%)	11/42 (26.2%)	40/215 (18.6%)	0.3	32/164 (19.5%)	19/93 (20.4%)	0.87

BED, biological effective dose.

patients (5.4%). The pulmonary symptoms resolved in most patients without steroid therapy, but six patients who had very poor respiratory function or severe pulmonary fibrosis before irradiation needed continuous oxygen. Chronic segmental bronchitis and wall thickening causing atelectasis in the peripheral lung was observed in one patient (0.4%). Transient grade 3 esophagitis was observed in two patients (0.8%) with tumors adjacent to the esophagus. Grade 3 or 4 dermatitis was observed in three patients (1.2%) with tumors adjacent to the chest wall. Rib fracture adjacent to the tumor was found in four patients (1.6%). No vascular, cardiac, or bone marrow complications had been encountered as of the last follow-up.

Recurrence

The recurrence rates of local, regional nodal, and distant lesions according to the BED and stage are listed in Table 2. The local recurrence rate was significantly lower for a BED of 100 Gy or more compared with a BED of less than 100 Gy (8.4 versus 42.9%, $p < 0.01$). For greater BED subgroups, the local recurrence rate was 11.8% for a BED of 120 Gy or more ($n = 93$) and 8.1% for a BED of 140 Gy or more ($n = 37$). The local recurrence rates for adenocarcinoma and squamous cell carcinoma were 13.3% (16/120) and 17.1% (19/111), respectively in 3 years. The cumulative local control rate curves according to BED subgroup are shown in Figure 2. The 5 (3? according to Table 2)-year local control rates of the BED of 100 Gy or more and less than 100 Gy subgroups were 84.2% (95% confidence interval [CI]: 77.7%–90.8%) and 36.5% (95% CI: 10.4%–62.6%), respectively. According to subgroup analysis, stage IB patients had a significantly higher rate of local recurrence than stage IA patients. The nodal and distant recurrence rates were almost identical in the stage IA and IB subgroups.

In the patients with regional nodal recurrence, nodal failures overlapped local failure in 3.1%, distant metastases in 3.9%, or both in 0.8% of the patients. Isolated local, nodal, and distant recurrences were observed in 8.6%, 5.1%, and 13.6% of the patients, respectively.

Survival

The overall 3- and 5-year survival rates for all patients were 56.8% (95% CI: 50.2%–63.5%) and 47.2% (95% CI: 38.7%–53.5%), respectively. The cause-specific 3- and 5-year survival rates were 76.9% (95% CI: 70.6%–83.2%) and 73.2% (95% CI: 66.1%–80.2%), respectively. The overall survival rates differed significantly according to medical operability, with intercurrent death in 36.8% of inoperable patients and 10.3% of operable patients. The overall 5-year survival rates of medically operable and inoperable patients (Figure 3) were 64.8% (95% CI: 53.6%–75.9%) and 35.0% (95% CI: 25.9%–44.1%), respectively. The overall survival rates according to the BED in all patients differed significantly between the BED of less than 100 Gy and 100 Gy or more subgroups. The overall 5-year survival rates of the BED 100 Gy or more and less than 100 Gy subgroups were 53.9% (95% CI: 46.0%–61.8%) and 19.7% (95% CI: 5.9%–33.4%), respectively. For the subgroup of medically operable patients with a BED of 100 Gy or more, the 3- and 5-year overall survival rates were 80.4% (95% CI: 71.0%–89.7%) and 70.8% (95% CI: 59.3%–82.2%), respectively (Figure 2). The overall 5-year survival rate according to stage in the operable patients irradiated with a BED of 100 Gy or more was 72.3%

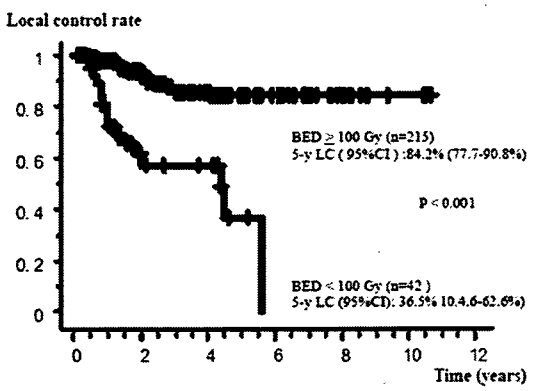

FIGURE 2. Cumulative local control rate according to the biological effective dose (BED). LC, local control rate; CI, confidence interval.

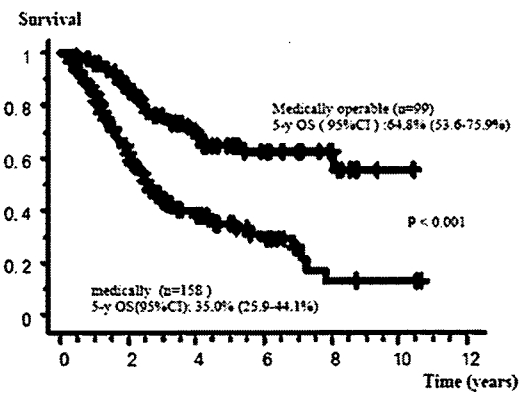

FIGURE 3. Overall survival rate according to medical operability. OS, overall survival rate; CI, confidence interval.

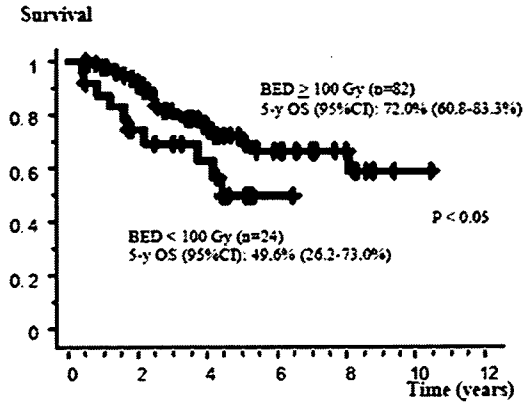

FIGURE 4. Overall survival rate in operable patients according to the biological effective dose (BED). OS, overall survival rate; CI, confidence interval.

(95% CI: 59.1%–85.6%) for stage IA and 65.9% (95% CI: 43.0%–88.9%) for stage IB patients (Figure 4).

Reproducibility of the Data Among Institutions

Table 3 compares the irradiation method and results for three major institutions enrolled in this study. These institutions used a BED of 100 Gy or more. The local control and 3-year survival rates were almost identical.

DISCUSSION

At present, surgery is the standard treatment for stage I NSCLC. RT is offered to patients who are unsuitable for surgery because of medical problems and to patients who refuse surgery. Most information on the results of RT for stage I NSCLC is based on retrospective studies of RT-treated inoperable NSCLC cases. Therefore, the role of RT for stage I NSCLC, as a curative modality, has not yet been established.

Qiao et al. summarized 18 papers on stage I NSCLC treated with conventional RT alone published between 1988 and 2000.[10] Local recurrence was the most common reason for treatment failure of stage I NSCLC with conventional RT, but the frequency of recurrence varied considerably according the report (between 6.4% and 70%). The 3-year recurrence rate was approximately 60%,[11–13] with a median time to relapse that ranged from 21 to 30 months.[12,14,15] Generally, smaller tumor size, low T stage, and increased dose had a favorable impact on local control, and increased local control was followed by increased survival.[14,16] However, the overall treatment results were disappointing. The median survival in these studies ranged from 18 to 33 months. The 3- and 5-year overall survival rates were 34 ± 9% and 21 ± 8% (mean ± 1 SE), respectively. The cause-specific survival rates at 3 and 5 years were 39 ± 10% and 25 ± 9% (mean ± 1 SE), respectively. Regarding treatment toxicity, severe (grade 3 or above) radiation esophagitis[14] and pneumonitis[11] occurred in 4.1% and 6.1% of the cases, respectively. Better local control may be achieved when the total dose is increased,[15,16] and a trend has been growing toward seeking better local control by increasing the BED[13–15] for a relatively limited span of doses (BED 59–76 Gy). Dose escalation has been the focus of developmental therapeutic strategies for inoperable stage I NSCLC to improve local control and survival.

Mehta et al.[17] provided a detailed theoretical analysis regarding the responses of NSCLC to RT and a rationale for dose escalation. They concluded that a greater BED irradiated during a short period must be given to gain local control of lung cancers. Giving a higher dose to the tumor without increasing the adverse effects was shown to be possible using the SRT technique; this is now feasible due to the technological progress that allows increasing the accuracy of localization to the tumor-bearing area using various imaging tools. SRT can also reduce the overall treatment time substantially, from several weeks for conventional RT to a few days, offering an important advantage to the patient.

After Uematsu et al.[18] reported a landmark study on SRT for stage I NSCLC using a CT-linac system, SRT has been actively investigated for stage I NSCLC in Japan and the United States. In the reports listed in Table 4,[3–6,19–21] the local control rates of primary lung cancer with SRT ranged from 87% to 97% when the BED exceeded 100 Gy. Uematsu et al.[3] showed excellent survival rates for medically operable patients, approximating those for full lobar surgical resection; however, they studied only a few patients, and it is not known whether the result is reproducible. Table 5 compares the results of Uematsu et al.[3] with the HypoFXSRT results presented here. These results suggest that the local control and survival rates of HypoFXSRT for stage I NSCLC are promising and reproducible when the BED exceeds 100 Gy.

In Japan, we consider a BED greater than 100 Gy to be a satisfactory dose for HypoFXSRT of stage I NSCLC, with a local control rate better than 85%, and a further dose escalation study is not necessary for tumors smaller than 4 cm in diameter. Conversely, in the United States, Timmerman et al.[22] concluded that 60 Gy in three fractions (BED = 180 Gy) is the proper dose, and they adopted this dose and fraction protocol for their prospective study. We need to observe the

TABLE 3. Comparison of the Irradiation Methods and Results for Three Major Institutions

Institution	No. of Patients	Total Isocenter Dose (Gy)	Single Isocenter Dose (Gy)	BED (Gy)	Median Follow-up (mo)	Local Failure, %	5-yr Overall Survival, %
Kyoto	42	48	12	106	40	3	64
Cancer Institute	30	50–62.5	10–12.5	100–141	25	4	77
Kitami	27	50–60	7.5–10	100–105	71	4	63

BED, biologically effective dose (α/β = 10) recalculated at the isocenter.

TABLE 4. Reports of Stereotactic Radiotherapy for Stage I Non-small Cell Lung Cancer

Author (ref.)	No. of Patients	Total Dose* (Gy)	Single Dose* (Gy)	BED† (Gy)	Median Follow-up (mo)	Local Progression, %	3-yr Overall Survival, %
Uematsu et al.[3]	50	72	7.2	124	60	6	66
Nagata et al.[4]	42	48	12	106	52	3	82
Fukumoto et al.[5]	17	48–60	6–7.5	99–137	24	6	NA
Onishi et al.[6]	28	72	7.2	124	24	8	75
Hof et al.[19]	10	19–26	19–26	55–94	15	20	NA
McGarry et al.[20]	47	75	25	263	15	13	NA
Wulf et al.[21]	12	26–57	19–26	94–165	11	5%	NA

BED, biologically effective dose; NA, not assessed.
*Stereotactic radiotherapy dose is calculated at the isocenter.
†BED (α/β = 10) recalculated at the isocenter.

results of ongoing phase II studies on SRT for stage I NSCLC conducted in Japan (12 Gy × 4 = 48 Gy prescribed to the isocenter) and the United States (20 Gy × 3 = 60 Gy prescribed to cover 95% of the PTV).

The 5-year overall survival rate for medically operable patients with HypoFXSRT is encouraging (Table 6). Representative 5-year overall survival rates for clinical stage IA and IB with surgery range from 61% to 72% and 40% to 50%, respectively.[23–25] According to our data, the survival rate for SRT was not worse than that for large surgical series. Furthermore, concerning toxicity, approximately 3% of patients died as a result of surgery, and chronic morbidity occurs in 10% to 15% of patients after surgery.[26] HypoFXSRT is much less invasive than surgery, and it is postulated that SRT will become a major treatment choice for stage I NSCLC, at least for medically inoperable patients.

TABLE 5. Comparison of the Results between the Multi-institutional Study and the Uematsu et al. Study

	Uematsu et al. [3]	Multi-institutional
Total no. of cases	50	215
T1N0M0	24	141
T2N0M0	26	75
Follow-up duration, mo (median)	22–66 (36)	2–128 (38)
Local control, %	94	90
Regional lymph nodes metastases, %	4	7
Distant metastases, %	14	19
Grade ≥3 toxicity, %	0	3
3-yr overall survival rate, %	66	64
3-yr cause-specific survival rate, %	88	83
5-yr overall survival rate, %	55	55
5-yr cause-specific survival rate, %	81	77
3-yr overall survival rate in operable patients, %	86	82
5-yr overall survival rate in operable patients, %	77	72

TABLE 6. Comparison of 5-Year Overall Survival Rate between Stereotactic Radiotherapy and Surgery

Stage	Author			
	Mountain[23]*	Naruke et al.[24]*	Shirakusa and Koybayashi[25]*	Onishi†
IA	61%	71%	72%	72%
IB	40%	44%	50%	66%

*Surgery.
†HypoFXSRT presented here.

Multi-institutional phase II studies of SRT for stage I NSCLC have been started in Japan (JCOG0403)[27] and the United States (RTOG0236).[28] However, it will take several years to obtain conclusive results, and an inevitable selection bias exists in comparing SRT with surgical series for patients in retrospective or phase II studies.

Although the differences in techniques and schedules of the institutions enrolled in this study may be large, it is meaningful that a safe, effective BED was suggested because the optimal dose-fraction schedule of SRT for stage I NSCLC is not known. Furthermore, this is the only report that gives the results of SRT for a large number of medically operable stage I NSCLC patients. Based on our excellent SRT results, it is arguable that a phase III study comparing surgery and SRT for medically operable patients is warranted. However, it is very difficult to perform a phase III study because most patients will opt for less invasive therapy such as SRT. We need much more experience and must study more patients with a longer follow-up duration to establish a safe, effective irradiation method that will instill both medical and social confidence in SRT for treatment of stage I NSCLC.

When we compare the results of conventional RT and surgery with those of HypoFXSRT, we conclude that HypoFXSRT has the following benefits for stage I NSCLC. First, HypoFXSRT is a safe and promising treatment modality. Second, the local control and survival rates are superior to those of conventional RT. Third, HypoFXSRT should be a standard of care for medically inoperable patients. Fourth, HypoFXSRT should be randomly compared with surgery for medically operable patients. Finally, we need additional experience with a longer follow-up duration to conclusively validate these points.

REFERENCES

1. Smythe WR. American College of Chest Physicians: treatment of stage I non-small cell lung carcinoma. *Chest* 2003;123:S181–S187.
2. Qiao X, Tullgren O, Lax I, et al. The role of radiotherapy in treatment of stage I non-small cell lung cancer. *Lung Cancer* 2003;41:1–11.
3. Uematsu M, Shioda A, Suda A, et al. Computed tomography-guided frameless stereotactic radiography for stage I non-small-cell lung cancer: 5-year experience. *Int J Radiat Oncol Biol Phys* 2001;51:666–670.
4. Nagata Y, Takayama K, Matsuo Y, et al. Clinical outcomes of a phase I/II study of 48 Gy of stereotactic body radiotherapy in 4 fractions for primary lung cancer using a stereotactic body frame. *Int J Radiat Oncol Biol Phys* 2005;63:1427–1431.
5. Fukumoto S, Shirato H, Shimizu S, et al. Small-volume image-guided radiotherapy using hypofractionated, coplanar, and noncoplanar multiple fields for patients with inoperable stage I nonsmall cell lung carcinomas. *Cancer* 2002;95:1546–1553.
6. Onishi H, Kuriyama K, Komiyama T, et al. Clinical outcomes of stereotactic radiotherapy for stage I non-small cell lung cancer using a novel irradiation technique: patient self-controlled breath-hold and beam switching using a combination of linear accelerator and CT scanner. *Lung Cancer* 2004;45:45–55.
7. Onishi H, Araki T, Shirato H, et al. Stereotactic hypofractionated high-dose irradiation for stage I nonsmall cell lung carcinoma. *Cancer* 2004;101:1623–1631.
8. Yaes RJ, Patel P, Maruyama Y. On using the linear-quadratic model in daily clinical practice. *Int J Radiat Oncol Biol Phys* 1991;20:1353–1362.
9. Therasse P, Arbuck SG, Eisenhauer EA, et al. New guidelines to evaluate the response to treatment in solid tumors. *J Natl Cancer Inst* 2000;92:205–216.
10. Qiao X, Tullgren O, Lax I, et al. The role of radiotherapy in treatment of stage I non-small cell lung cancer. *Lung Cancer* 2003;41:1–11.
11. Sibley GS. Radiotherapy for patients with medically inoperable stage I nonsmall cell lung carcinoma. *Cancer* 1998;82:433–438.
12. Cheung PC, Mackillop WJ, Dixon P, et al. Involved-field radiotherapy alone for early-stage non-small-cell lung cancer. *Int J Radiat Oncol Biol Phys* 2000;48:703–710.
13. Hayakawa K, Mitsuhashi N, Saito Y, et al. Limited field irradiation for medically inoperable patients with peripheral stage I non-small cell lung cancer. *Lung Cancer* 1999;26:137–142.
14. Jeremic B, Shibamoto Y, Acimovic YL, et al. Hyperfractionated radiotherapy alone for clinical stage I non-small cell lung cancer. *Int. J. Radiat Oncol Biol Phys* 1997;38:521–525.
15. Kaskowitz L, Graham MV, Emami B et al. Radiation therapy alone for stage I non-small cell lung cancer. *Int J Radiat Oncol Biol Phys* 1993;27:517–523.
16. Kupelian PA, Komaki R, Allen P. Prognostic factors in the treatment of node-negative non-small cell lung carcinoma with radiotherapy alone. *Int J Radiat Oncol Biol Phys* 1996;36:607–613.
17. Mehta M, Scringer R, Mackie R, et al. A new approach to dose escalation in non-small cell lung cancer. *Int J Radiat Oncol Biol Phys* 2001;49:23–33.
18. Uematsu M, Shioda A, Tahara K, et al. Focal, high dose, and fractionated modified stereotactic radiation therapy for lung carcinoma patients: a preliminary experience. *Cancer* 1998;82:1062–1070.
19. Hof H, Herfarth KK, Munter M, et al. Stereotactic single-dose radiotherapy of stage I non-small cell lung cancer. *Int J Radiat Oncol Biol Phys* 2001;49:23–33.
20. McGarry RC, Papiez L, Williams M, et al. Stereotactic body radiotherapy of early-stage non-small cell lung carcinoma: phase I study. *Int J Radiat Oncol Biol Phys* 2005;63:1010–1015.
21. Wulf J, Hadinger U, Oppitz U, et al. Stereotactic radiotherapy for primary lung cancer and pulmonary metastases: a noninvasive treatment approach in medically inoperable patients. *Int J Radiat Oncol Biol Phys* 2004;60:186–96.
22. Timmerman R, Papiez L, McGarry R, et al. External stereotactic radioablation: results of a phase I study in medically inoperable stage I non-small cell lung cancer patients. *Chest* 2003;124:1946–1955.
23. Mountain CF. The international system for staging lung cancer. *Semin Surg Oncol* 2000;18:106–115.
24. Naruke T, Tsuchiua R, Kondo H, et al. Prognosis and survival after resection for bronchogenic carcinoma based on the 1997 TNM-staging classification: the Japanese experience. *Ann Thorac Surg* 2001;71:1759–1764.
25. Shirakusa T, Kobayashi K. Lung cancer in Japan: analysis of lung cancer registry for resected cases in 1994. *Jpn J Lung Cancer* 2002;42:555–562.
26. Deslauriers J, Ginsberg RJ, Dubois P, et al. Current operative morbidity associated with elective surgical resection for lung cancer. *Can J Surg* 1989;32:335–339.
27. http://www.clinicaltrials.gov/ct/show/NCT00238875.
28. http://www.rtog.org/members/protocols/0236/0236.pdf.

Radiat Med (2007) 25:453–461
DOI 10.1007/s11604-007-0165-z

ORIGINAL ARTICLE

Experimental stereotactic irradiation of normal rabbit lung: computed tomographic analysis of radiation injury and the histopathological features

Takatsugu Kawase · Etsuo Kunieda · Hossain M. Deloar
Satoshi Seki · Akitomo Sugawara · Takanori Tsunoo
Eileen N. Ogawa · Akitoshi Ishizaka · Kaori Kameyama
Atsuya Takeda · Atsushi Kubo

Received: March 20, 2007 / Accepted: June 18, 2007

Abstract
Purpose. The aim of this study was to establish an animal experimental model of pulmonary stereotactic irradiation and clarify the morphological patterns of pulmonary radiation injury with computed tomography and the histopathological features.
Materials and methods. Tiny spherical regions in the lungs of seven anesthetized rabbits were irradiated stereotactically with a single fractional dose of 21–60 Gy. Subsequently, the irradiated lungs were observed biweekly with computed tomography (CT) for 24 weeks. Radiation injury of the lung was examined histopathologically in one specimen.
Results. Localized hypodense changes were observed 7–15 weeks after irradiation in three rabbits irradiated with 60 Gy, and the findings persisted beyond that time. The electron density ratios in the lung fields obtained from the CT images were shown to be decreasing, corresponding to the hypodensity changes. No clear increased density opacity was observed in any rabbit in the 60-Gy irradiated group. Severe localized fibrotic change was observed in the histopathological specimens.
Conclusion. Specific localized hypodensity changes were found in only three rabbits irradiated with 60 Gy, the highest dose we employed.

Key words Stereotactic radiotherapy · Rabbit · Lung · Computed tomography · Radiation injury

T. Kawase · E. Kunieda (✉) · S. Seki · A. Sugawara · T. Tsunoo · A. Kubo
Department of Radiology, Keio University School of Medicine, 35 Shinanomachi, Shinjuku-ku, Tokyo 160-8582, Japan
Tel. +81-3-5363-3835; Fax +81-3-3359-7425
e-mail: kunieda@sc.itc.keio.ac.jp

T. Kawase · E. Kunieda · T. Tsunoo
CREST, Japan Science and Technology Agency, Tokyo, Japan

H.M. Deloar
Oncology Service, Medical Physics and Bioengineering Department, Christchurch Hospital, Christchurch, New Zealand

E.N. Ogawa
Department of Anesthesiology, Keio University School of Medicine, Tokyo, Japan

A. Ishizaka
Department of Medicine, Keio University School of Medicine, Tokyo, Japan

K. Kameyama
Division of Diagnostic Pathology, Keio University School of Medicine, Tokyo, Japan

A. Takeda
Radiotherapy Department, Ofuna Chuuo General Hospital, Kanagawa, Japan

Introduction

Hypofractionated stereotactic radiotherapy of early non-small-cell lung carcinoma is developing as a minimally invasive treatment. Compared to conventional radiotherapy, such as with rectangular coplanar portals with a usual fractional dose, the new method can provide a higher dose and concentration of irradiation of a localized tumor. Considerable clinical experience and favorable outcomes have been reported.[1]

The dose prescriptions of the irradiation method are controversial;[2–4] however, the biological effective doses (BEDs)[5] calculated from these reports were similar to ensure clinical safety. Koenig et al.[6] categorized computed tomography (CT) findings of radiation injury induced with hypofractionated three-dimensional radio-

therapy, and subsequently Takeda et al.[7] also analyzed by CT the radiation injury induced with hypofractionated stereotactic radiotherapy of human lung tumors. The patients described in these articles were irradiated with the dose prescription described above. These studies clarified only the patterning of radiation injury induced with the same dose prescription; therefore, the variety of the CT findings arising from differences of BED was not mentioned. This lack of information led us to study the dose dependence of radiation injury during stereotactic irradiation of animal lungs. As for an attempt to examine morphological changes of animal extracranial viscera induced with focused single-high dose irradiation, Herfarth et al.[8] formerly reported experimental single coplanar rotational irradiation to normal rabbit liver; however, in their article none of the changes in the irradiated liver were documented by CT images or in histopathological specimens.

In this investigation, we attempted to establish an experimental technique for irradiating stereotactically a tiny spherical partial volume of normal rabbit lung with a linear accelerator and for examining the induced radiation injury with a CT scanner. This is the first report of stereotactic irradiation of rabbit lung. We report the CT characteristics of acute and subacute radiation injury generated with varied single-fractional-dose stereotactic irradiation in the lungs of seven rabbits. Histopathological findings in one rabbit lung irradiated with 60 Gy as a single fractional dose are also mentioned.

Materials and methods

Preparation

Institutional guidelines for the care and use of laboratory animals were followed in all experiments, and the use of rabbits was approved.

Seven Japanese White Rabbits (all male, weighing 2.9–3.2 kg) were used. In all procedures of this experiment, the rabbits were anesthetized with 100 mg ketamine hydrochloride intramuscularly and with continuous intravenous injections of pentobarbital sodium at 20 mg/kg/h.

Each rabbit was immobilized on a vacuum-forming patient-holding pillow (Vacufix; Muranaka Medical Instruments, Osaka, Japan) in a supine position in a wooden box. On the top and lateral surfaces of the box, straight aluminum wires were attached diagonally to measure the three-dimensional coordinates in the box on the CT images.

Irradiation

Each rabbit was scanned with a CT simulator machine (Xvision GX, TSX-002A; Toshiba Medical Systems, Tokyo, Japan), and the beam isocenter was aimed at the peripheral point adjacent to the left lung base center. The isocenter was placed on the point so the effect of pulmonary respiratory movement would be minimal as verified by fluoroscopic observation. The side beam marker points were marked on the surface of the wooden box containing the rabbit, which was positioned on the couch of the X-ray linear accelerator.

A partial spherical volume centered on the isocenter was irradiated stereotactically by 4 MV of X-ray energy in a narrow rectangular beam (11 × 11 mm) with a linear accelerator. Three noncoplanar arcs (couch rotation: –45°, 0°, +45°) were used for arc rotation. Each gantry rotation arc was 160° to avoid opposing beams.

The irradiation was done in a single fraction in 1 day. Each rabbit received a different total irradiated dose. The doses were 21, 30, 39, 48, 60, 60, and 60 Gy. Each dose was normalized at the beam isocenter. The dose distributions and monitor units of irradiation were calculated using the Batho power law algorithm[9] as an inhomogeneity correction on a Eclipse radiotherapy planning system (Varian Medical Systems, Palo Alto, CA, USA) (Fig. 1). The irradiated volumes of the rabbit lungs using the irradiation plan were shown as a dose–volume histogram (Fig. 2). The doses of irradiation were also estimated using convolution and superposition dose calculation algorithms from the actual irradiated dose monitor units (Table 1). These algorithms were applied with Focus XiO version 4.2 (CMS, St. Louis, MO, USA).

CT scanning

All rabbits were examined for 24 weeks after irradiation. Each rabbit was scanned with a CT scanner (Toshiba Aquilion, TSX-101A; Toshiba Medical Systems) approx-

Table 1. Actual irradiated doses calculated with Batho power law algorithm and corresponding doses estimated with convolution and superposition algorithms

Irradiated dose (Gy)	Estimated dose (Gy)	
Batho power law	Convolution	Superposition
60.00	54.23	55.78
48.00	43.39	44.63
39.00	35.25	36.26
30.00	27.12	27.89
21.00	18.98	19.52

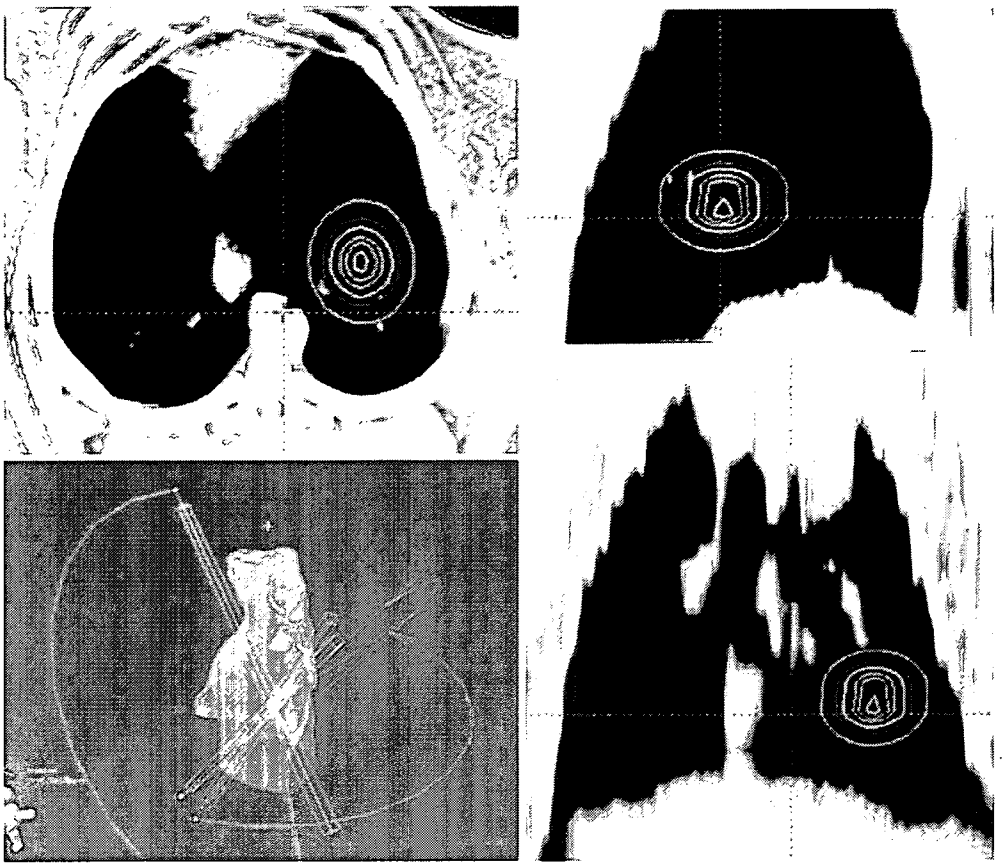

Fig. 1. Beam configuration (*bottom left*) and other isodose distributions. The isodose lines represent 100%, 95%, 90%, 80%, 70%, 50%, respectively (from the inside)

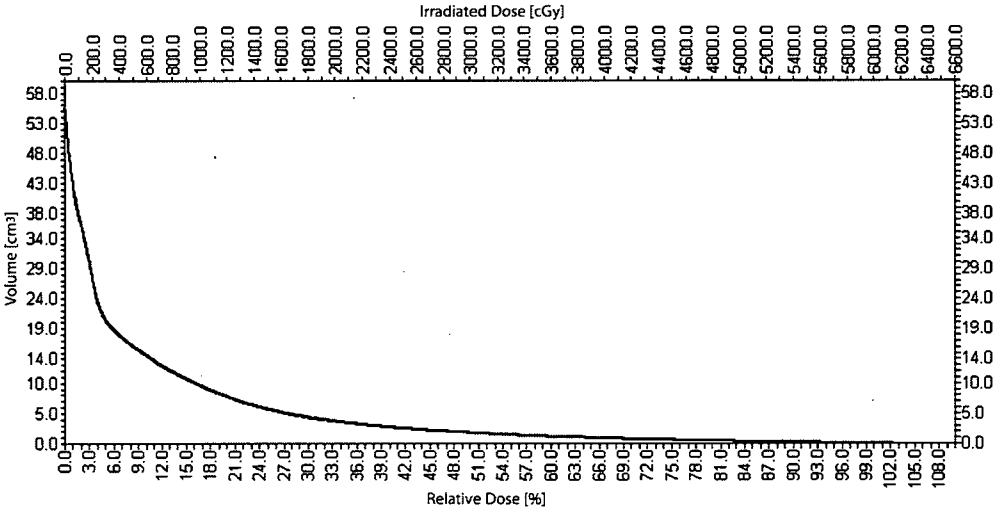

Fig. 2. Dose-volume histogram of the whole lung. Vertical axis represents the lung volume that receives a dose greater than or equal to a specified dose. Horizontal axis represents the cumulative dose. The total volume of whole rabbit lung was 55.4 cm^3. The lung volumes irradiated with >100%, 90%, 70%, and 50% of the prescribed dose were 0.01, 0.16, 0.69, and 1.74 cm^3, respectively

imately biweekly, and the image data were collected as Digital Imaging and Communications in Medicine (DICOM) standard files. The CT images were scanned with a slice thickness of 2 mm and helical pitch of 1. All rabbits were under intravenous general anesthesia with the method as described above during the CT scanning procedures.

CT image analysis

The image data were transferred to a workstation via a local area network and were analyzed by a radiologist visually for detecting hyperdense or hypodense changes deviating from the normal CT appearance in the lung fields.

The data were also analyzed by technical computing language software (MATLAB version 7.2.0.232; The Mathwork, Natick, MA, USA). Initially, the pixel values of the CT images were converted from Hounsfield units (HU) to electron density. For the procedure, a converting formula[10] was used as follows:

$$\rho = 1.000 + 0.001\ N_{CT} \quad \text{for} \quad -1000 \leq N_{CT} \leq 100$$

where ρ is the electron density of tissue relative to water, and N_{CT} (CT number) is the Hounsfield unit.

In the electron density image at the beam isocenter, two round regions of interest (ROIs) 11 mm in diameter were delineated. One corresponded to the stereotactically irradiated area (ROI A), and the other was placed on the same part of the contralateral lung (ROI B) (Fig. 3).

The mean electron density of all the pixels in each ROI was calculated and their ratios (ROI A/ROI B) were determined. These calculations were performed for all the acquired CT images. The electron density ratios were plotted for examining the time-evolution tendency.

Histopathological observations

One of the rabbits irradiated with 60 Gy was killed with an intravenous injection of an excessive dose of pentobarbital sodium 489 days (69 weeks) after irradiation, and the whole lung with trachea was obtained as a pathological specimen. Formaldehyde solution (10%) was added through the trachea with positive pressure to fill the pulmonary air cavity. The fixed lung was observed macroscopically and then was embedded in paraffin. Thin-slice sections were cut, stained with hematoxylin-eosin (H&E), and were examined with an optical microscope.

Results

Computed tomographic analysis

Table 2 shows the timing and acquired findings of rabbit chest CT examinations conducted for 24 weeks after irradiation. Overall, only slight changes were observed in the irradiated lungs. Localized hypodense changes suggesting emphysematous change appeared 7–15 weeks after irradiation in the parts of the three rabbits irra-

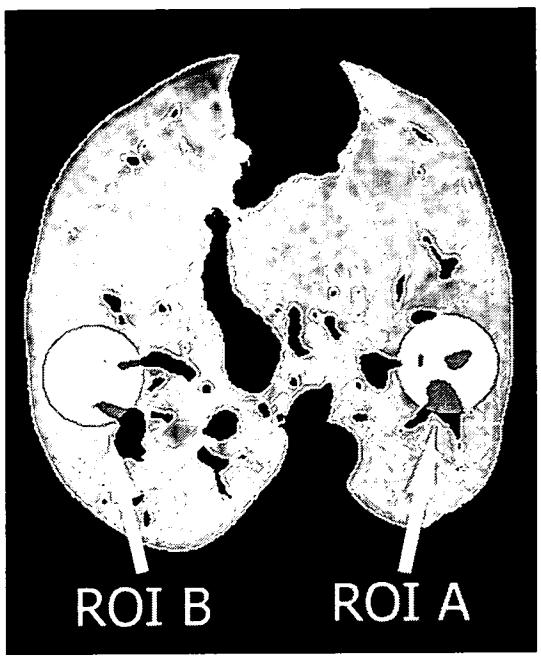

Fig. 3. Computed tomographic (CT) analysis of electron density changes in irradiated rabbit lungs. The region of interest, irradiated area (*ROI A*) and that of corresponding area in the contralateral lung (*ROI B*) were delineated. The mean electron density of each area was calculated with MATLAB software

Table 2. Radiographic follow-up timing with computed tomography and the findings observed in each irradiated rabbit

Rabbit no.	Irradiated Dose (Gy)	Interval after irradiation (weeks)																							
		0		2		4		6		8		10		12		14		16		18		20		22	24
1	60	–		–	–	–	–	–	#	#	#	#	#	#	#	#	#	#		#	#	#	#	#
2	60	–		–	–	–	–	–	#	#	#	#	#	#	#	#	#	#		#	#	#	#	#
3	60	–		–	+	–	–	–	–	+	–	–	–	–	–	–	#	#		#	#	#	#	#
4	48	–	–	–		–		–		–	–	–	–	–	–	–		–		–	–	–	–	–
5	39	–		–		–		–		–		–		–		–		+	–	–	–	–	–	–
6	30	–	–	–	–	–		–		+	+	+	–	–		–	–	–		–	–	–	–	–
7	21	–		–			–	–		–		–		–		–		–		–	–	–	–	–

#, Localized hypodense change; +, localized increased opacity; –, nothing particular

diated with 60 Gy (Fig. 4). The findings persisted throughout the experimental period after the first visualization.

As shown in Table 2, localized increased opacities were observed 3–16 weeks after irradiation in only three rabbits irradiated with 30, 39, and 60 Gy. The findings were slight (Fig. 5), persisted for only 1–3 weeks, and then vanished. Two rabbits irradiated with 21 and 48 Gy did not have any significant findings.

The time evolutions of electron density ratios of two roundly delineated areas in the rabbit lung fields are shown in Fig. 6. In the 60-Gy group, there is a marked decrease of the electron density ratios that corresponds to the localized hypodense changes observed 6–7 weeks after irradiation. No remarkable decreases were observed in the rabbits irradiated with ≤48 Gy.

Histopathological findings

Severe localized fibrotic and scarring were observed on the parietal pleural surface toward the central area of the lung field (Fig. 7). In the fibrotic area showing contracture of the overlying pleura (Fig. 8), there was thickening of alveolar septa and narrowing of air cavities (Fig. 9). Localized ossification was observed away from the center of the major localized fibrotic change. Mild concentric thickening of the small arteries and scattered foreign body giant cells were also identified.

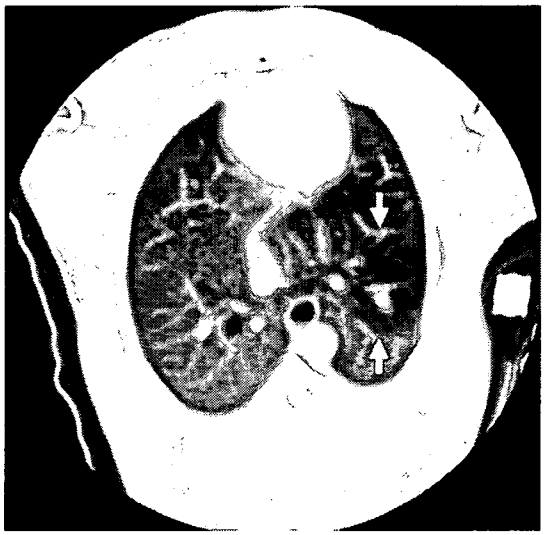

Fig. 4. Localized hypodense change appeared in rabbit lung irradiated with a single fractional dose of 60 Gy 11 weeks after irradiation (*arrows*)

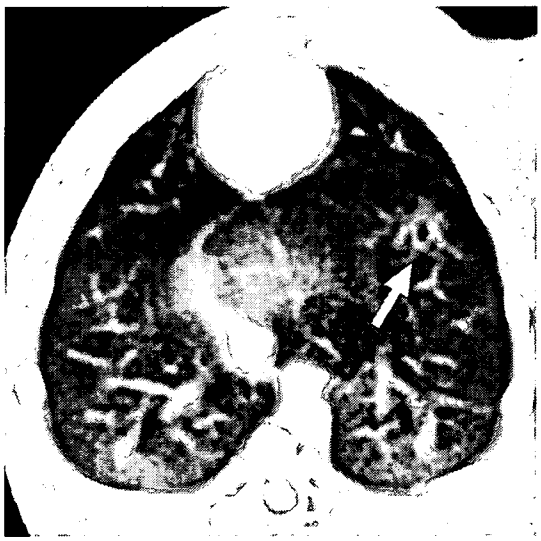

Fig. 5. Slight localized increased opacity in rabbit lung irradiated with a single fractional dose of 30 Gy 10 weeks after irradiation (*arrow*)

Fig. 6. Time evolution of the electron density ratio (ROI A/ROI B), which was calculated for each scanned rabbit lung image

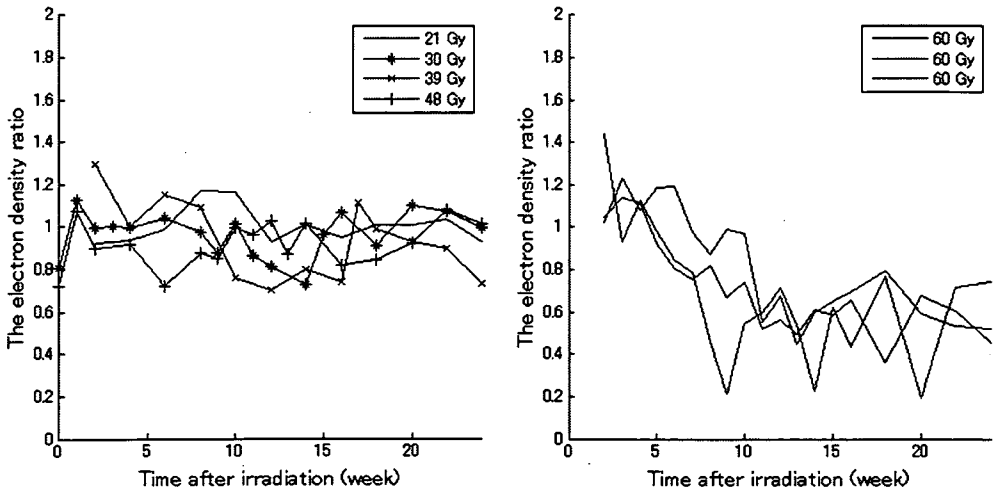

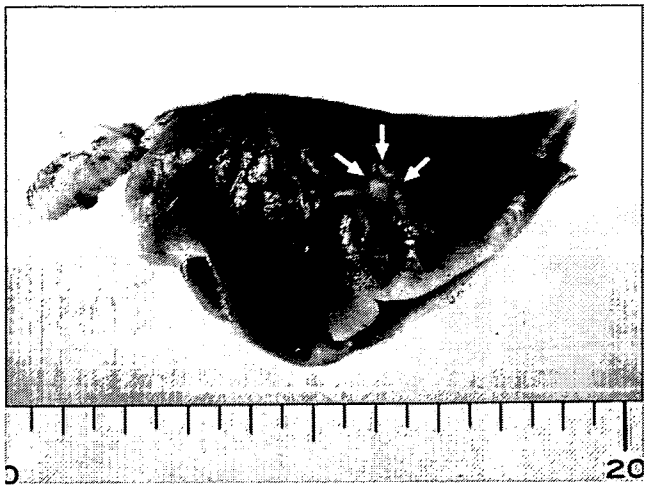

Fig. 7. Macroscopic appearance of rabbit lung irradiated with a single dose of 60 Gy obtained 69 weeks after irradiation. Severe localized scarring appears on the pleural aspect near the irradiation target (*arrows*)

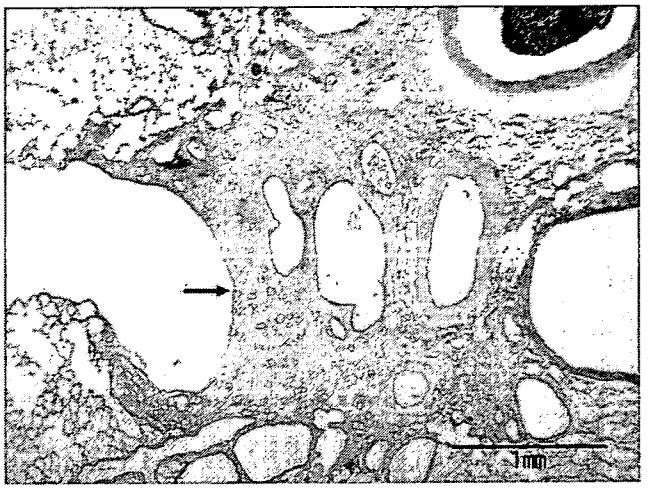

Fig. 9. High-power field focused on the area depicted by the *gray arrow* in Fig. 8. There is marked local thickening of the alveolar and vessel walls. These changes are localized (*black arrow* points the pleural aspect). (H&E)

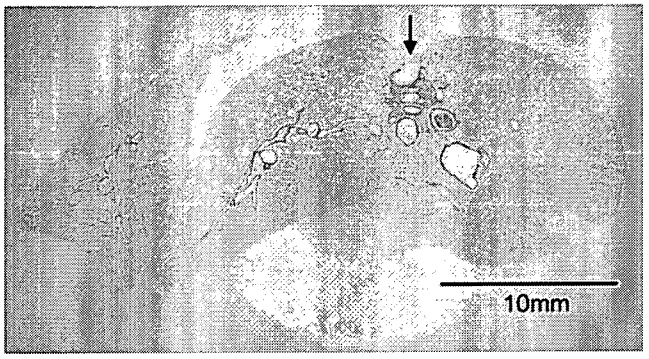

Fig. 8. Histopathological specimen of rabbit lung irradiated with a single dose of 60 Gy obtained 69 weeks after irradiation. Note the severe fibrotic change continuing from the pleural aspect (*arrow*). (H&E, low-power field)

Discussion

Our study was inspired by the recent retrospective CT analysis of radiation injury after stereotactic or three-dimensional conformal irradiation of a human lung. Takeda et al.[7] reported the CT manifestations of serial changes from pulmonary radiation injury after hypofractionated stereotactic irradiation for lung tumors. The irradiation dose generally consisted of 50 Gy in five fractions administered over 5–7 days. As a result, ground-glass opacities were observed around 4 (18%) of 22 lesions 3–6 months after irradiation. Increased density opacities, including dense consolidation, on or near the irradiated areas were observed in 16 (73%) of 22 target lesions within 6 weeks after irradiation. Koenig et al.[6] identified pulmonary ground-glass opacities in all (100%) seven patients who underwent CT scanning within 3 months after irradiation. Aoki et al.[11] detected increased density opacities (chiefly patchy consolidation) within 2–6 months after irradiation in all 31 lesions irradiated stereotactically. Based on these reports, it is likely that certain increased density opacities in human lungs will be observed in high frequency on CT scans within 6 months after stereotactic irradiation.

We expected to acquire new knowledge of radiation injury induced with single high-dose stereotactic irradiation of normal rabbit lung. We believe our study is the first one using pulmonary stereotactic irradiation using such an animal model. Localized hypodense change corresponding to the irradiated target was observed in each lung irradiated with 60 Gy as a single dose. However, minimal changes were observed during the observation period in the lungs irradiated with 48 Gy and lower doses. As a whole, no major increased opacities were detected in any of the irradiated lungs. Therefore, we focus on our two findings about localized hypodense change and increased density opacity.

Localized hypodense change is a new finding. In the retrospective human study cited above, this finding was not described. We did not examine the rabbit lung histopathologically at the site of the change because we needed to perform additional CT imaging examinations. Although the histopathology of the opacity was not clarified, hypodense changes on CT images are known to represent emphysematous change.[12] This change had specific morphology that expanded over the spherical target volume that was about 1 cm in diameter and extended to the subpleural area. It has been noted that

the increased opacity due to stereotactic irradiation of human lung also extends to the subpleural area;[7] therefore, the existence of a common mechanism for development of subpleural opacity can be predicted. This finding may possibly be found on CT images of lungs irradiated stereotactically with higher single doses as therapeutic doses are escalated.

We compared the features of the CT findings of increased density opacity in this study with those of the human changes reported in the literature.[6,7] Increased density opacities arising in the acute and subacute phases are categorized as ground-glass, consolidation, and linear opacities. Our experiments showed only transient and slight localized increased opacities in three of seven rabbits. Rabbit lung might be more tolerant of irradiation than human lung;[13] however, previous rabbit experiments[14–17] have documented severe radiation reactions due to broad photon beam irradiation. This discrepancy cannot be explained as a species difference, so further research is needed.

We also studied the CT findings with MATLAB software on a workstation to evaluate pulmonary parenchymal changes numerically. It was revealed that the electron densities of the lung field irradiated with 60 Gy were gradually decreasing nearly corresponding to the appearance of localized hypodensity changes on the CT images. In contrast, no remarkable hyperdense opacity was seen. Although an increase of CT numbers reflecting the increased density of the lung field after irradiation was reported in a similar experiment using a mouse model,[18] such a tendency was not apparent in our experiment.

About 16 months after irradiation with 60 Gy in a single dose, severe localized pulmonary fibrotic change, centric thickenings of the vessel intima, and tiny ossifications were observed. These histopathological findings were similar to those following pulmonary radiation injury induced with broad photon beams;[13] however, their localized and severe expression were specific in our results. No radiation injury was detected apart from the targeted volume in our work. These findings suggest the existence of a threshold dose for severe pulmonary fibrotic change. The fact that the severe fibrotic change continued to the visceral pleural aspect may be due to the pathological mechanisms that produced localized hypodense change in our study or subpleural increased opacity observed in human lungs.

The results of documented animal experiments should be considered. Experiments were reported in which rabbit lungs were radiographically observed following irradiation with photon beams. In these experiments, a large volume of the lung was irradiated with whole- or hemi-lung irradiation.[14–17] Resl et al.[15] administered single-dose irradiation of 24 Gy to whole lungs. They reported that pulmonary radiation injuries were observed within 2–3 weeks after irradiation. Hermann et al.[16] irradiated rabbit hemi-lungs with 38 Gy. The dose was administered in five fractions over 5 weeks. They reported that acute pulmonary injury was detected in 9 (37%) of 24 rabbits at 2–18 weeks after irradiation. In sum, these authors demonstrated that radiation injury of rabbit lung was generated with standard photon beams at a high rate; hence, their results differ from ours, where we used stereotactic irradiation to small target volumes in rabbit lungs.

The dose prescriptions for three conditions (human studies, our current study, past rabbit studies) described above can be evaluated by BEDs, calculated using the linear-quadratic model of Fowler.[5] The formula is not usually applicable to a high-dose single fraction above 23 Gy;[19] however, we expediently use it for comparison here. Although the α/β ratios have not been decided definitively, we propose 10 and 3 Gy for early and late lung injury, respectively. Species difference is not considered in this calculation. Under these assumptions, calculated BEDs for the rabbit lung irradiation experiments cited above have a range of 66.9–130.7 Gy_{10} for acute pulmonary injury and 103.3–362.3 Gy_3 for late pulmonary injury. The fractional doses prescribed in our experiments ranged from 21 to 60 Gy, which correspond to 65.1–420.0 Gy_{10} and 168.0–1260.0 Gy_3. The prescribed median dose of 48 Gy is equal to 278.4 Gy_{10} or 816.0 Gy_3, both of which exceed the values calculated with the doses cited above. Nevertheless, acute pulmonary radiation injury was slight in our experiment.

We did not evaluate functional changes of the rabbit lung after irradiation; however, we do not think this information is important in view of the slight CT changes. CT analysis of radiation injury is known to be more sensitive than pulmonary function tests.[20] Additionally, Ohashi et al.[21] reported minimal functional changes after stereotactic radiotherapy of human lung.

The question might arise whether the minimal acute and subacute radiation reactions on the CT images of the rabbit lungs in this study are due to the lack of irradiation accuracy. If the accuracy cannot be guaranteed, the irradiation dose on the target volume could be reduced. We have three reasons to dismiss this issue. First, we set the target volume center apart from the diaphragm and eliminated the effect of respiratory movement. The advantage was confirmed fluoroscopically. Second, we observed the small target respiratory movement with real-time CT dynamic mode. Finally, our histopathological findings ensure the accuracy of the irradiation. Therefore, dose reduction due to pulmonary respiratory movement can be ignored.

We should point out that the target objects were normal rabbit lungs. In the clinic, the target volume irradiated contains nodular malignant lesions. Therefore, rabbit lungs that had such a lesion should have been used in the experiment. We considered two methods for producing an artificial tumor in the rabbit lung, but neither was useable. First, a technique producing artificial pulmonary metastatic tumors by intravenous injection was evaluated.[22] In this model, the tumor could not be implanted in a specific point and tumor growth during the experimental period could not be predicted. Second, we designed a technique for percutaneous injection of malignant tumor cells or water-equivalent density material into rabbit lung. This method would induce pulmonary parenchymal density changes, and it would interfere with the CT observation of irradiated lungs. For these reasons, naive rabbit lungs were used as the irradiation objects.

The discrepancy of our results with the clinical experience should be pointed out, but we believe that our results may be applicable as a model mimicking certain kinds of human pulmonary malignancies, especially early lung adenocarcinoma presenting slight ground-glass opacity, highly differentiated adenocarcinoma, and bronchoalveolar adenocarcinoma. They are histopathologically known to be rich in air and to have slight destructive changes in the existing structure of the lung, particularly alveolar septa, bronchioles, and blood vessels.[23] Thus, our study has a similarity to a clinical subset of lung malignancy.

Conclusion

Specific and new localized hypodense changes were observed in only three rabbits irradiated with 60 Gy, the highest dose we employed. Rabbit lung might be more tolerant to acute and subacute radiation effects of single-fraction stereotactic radiotherapy than other animals' lungs because no major radiographic hyperdense changes could be observed.

Acknowledgments. Financial support was received from CREST/ Japan Science and Technology Agency.

References

1. Onishi H, Araki T, Shirato H, Nagata Y, Hiraoka M, Gomi K, et al. Stereotactic hypofractionated high-dose irradiation for stage I nonsmall cell lung carcinoma: clinical outcomes in 245 subjects in a Japanese multiinstitutional study. Cancer 2004;101:1623–31.
2. Nagata Y, Negoro Y, Aoki T, Mizowaki T, Takayama K, Kokubo M, et al. Clinical outcomes of 3D conformal hypofractionated single high-dose radiotherapy for one or two lung tumors using a stereotactic body frame. Int J Radiat Oncol Biol Phys 2002;52:1041–6.
3. Lee SW, Choi EK, Park HJ, Ahn SD, Kim JH, Kim KJ, et al. Stereotactic body frame based fractionated radiosurgery on consecutive days for primary or metastatic tumors in the lung. Lung Cancer 2003;40:309–15.
4. Hof H, Herfarth KK, Munter M, Hoess A, Motsch J, Wannenmacher M, et al. Stereotactic single-dose radiotherapy of stage I non-small-cell lung cancer (NSCLC). Int J Radiat Oncol Biol Phys 2003;56:335–41.
5. Fowler JF. Fractionation and therapeutic gain. In: Steel G, Adams GE, Peckham M, editors. The biological basis of radiotherapy. Amsterdam: Elsevier Science; 1983. p. 181–94.
6. Koenig TR, Munden RF, Erasmus JJ, Sabloff BS, Gladish GW, Komaki R, et al. Radiation injury of the lung after three-dimensional conformal radiation therapy. AJR Am J Roentgenol 2002;178:1383–8.
7. Takeda T, Takeda A, Kunieda E, Ishizaka A, Takemasa K, Shimada K, et al. Radiation injury after hypofractionated stereotactic radiotherapy for peripheral small lung tumors: serial changes on CT. AJR Am J Roentgenol 2004;182: 1123–8.
8. Herfarth KK, Munter MW, Groene HJ, Delorme S, Peschke P, Debus J. Absence of tissue reaction after focal high-dose irradiation of rabbit liver. Acta Oncol 2006;45:865–9.
9. Batho HF. Lung corrections in cobalt 60 beam therapy. J Can Assoc Radiol 1964;15:79–83.
10. Van Dyk J, Keane TJ, Rider WD. Lung density as measured by computerized tomography: implications for radiotherapy. Int J Radiat Oncol Biol Phys 1982;8:1363–72.
11. Aoki T, Nagata Y, Negoro Y, Takayama K, Mizowaki T, Kokubo M, et al. Evaluation of lung injury after three-dimensional conformal stereotactic radiation therapy for solitary lung tumors: CT appearance. Radiology 2004;230: 101–8.
12. Coddington R, Mera SL, Goddard PR, Bradfield JW. Pathological evaluation of computed tomography images of lungs. J Clin Pathol 1982;35:536–40.
13. Fajardo LF, Berthrong M, Anderson RE. Lung: radiation pathology. New York: Oxford University Press; 2001. p. 198–208.
14. Bellet M, Barthelemy L, Labat JP, Gendre P, Bardou L. Experimental study of the effect of cobalt irradiation on the rabbit lung. J Radiol Electrol Med Nucl 1975;56:749–60.
15. Resl M, Petyrek P, Kuna P. Morphological changes in the lungs after single whole-body irradiation in rabbits. Radiobiologiia 1987;27:532–5.
16. Hermann HJ, Wetzel E, Heller M, Hofmann W. Comparative investigations (computed tomography, X-ray diagnostics, scintigraphy) for the detection of radiation-induced alterations of the lung (author's transl). Strahlentherapie 1980; 156:248–52.
17. Schnabel K, Siegl R, Abel U, Hofmann W. Comparison of clinical methods for the demonstration of radiation-induced lung changes: experimental study on animals. Rofo 1983; 138:235–8.
18. Plathow C, Li M, Gong P, Zieher H, Kiessling F, Peschke P, et al. Computed tomography monitoring of radiation-induced lung fibrosis in mice. Invest Radiol 2004;39:600–9.
19. Fowler JF, Tomé WA, Fenwick JD, Mehta MP. A challenge to traditional radiation oncology. Int J Radiat Oncol Biol Phys 2004;60:1241–56.

20. Bentzen SM, Skoczylas JZ, Bernier J. Quantitative clinical radiobiology of early and late lung reactions. Int J Radiat Biol 2000;76:453–62.
21. Ohashi T, Takeda A, Shigematsu N, Kunieda E, Ishizaka A, Fukada J, et al. Differences in pulmonary function before vs. 1 year after hypofractionated stereotactic radiotherapy for small peripheral lung tumors. Int J Radiat Oncol Biol Phys 2005;62:1003–8.
22. Funakoshi N, Onizuka M, Yanagi K, Ohshima N, Tomoyasu M, Sato Y, et al. A new model of lung metastasis for intravital studies. Microvasc Res 2000;59:361–7.
23. Noguchi M, Morikawa A, Kawasaki M, Matsuno Y, Yamada T, Hirohashi S, et al. Small adenocarcinoma of the lung: histologic characteristics and prognosis. Cancer 1995;75:2 844–52.

Radiat Med (2007) 25:309–314
DOI 10.1007/s11604-007-0140-8

TECHNICAL NOTE

Interface software for DOSXYZnrc Monte Carlo dose evaluation on a commercial radiation treatment planning system

**Etsuo Kunieda · Hossain M. Deloar · Shunji Takagi
Koichi Sato · Takatsugu Kawase · Hidetoshi Saitoh
Kimiaki Saito · Osamu Sato · Graham Sorell
Atsushi Kubo**

Received: December 7, 2006 / Accepted: February 6, 2007

Abstract
Purpose. As the conventional graphical user interface (GUI) associated with DOSXYZnrc or BEAMnrc is unable to define specific structures such as gross tumor volume (GTV) on computed tomography (CT) data, the quantitative analysis of doses in the form of dose-volume histograms (DVHs) is difficult. The purpose of this study was to develop an interface that enables us to analyze the results of DOSXYZnrc output with a commercial radiation treatment planning (RTP) system and to investigate the validity of the system.
Materials and methods. Interface software to visualize three-dimensional radiotherapy Monte Carlo (MC) dose data from DOSXYZnrc on the XiO RTP system was developed. To evaluate the interface, MC doses for a variety of photon energies were calculated using the CT data of a thorax phantom and a uniform phantom as well as data from patients with lung tumors.
Results. The dose files were analyzed on the XiO RTP system in the form of isodose distributions and DVHs. In all cases, the XiO RTP system perfectly displayed the MC doses for quantitative evaluation in the form of differential and integral DVHs.
Conclusion. Three-dimensional display of DOSXYZnrc doses on a dedicated RTP system could provide all the existing facilities of the system for quantitative dose analysis.

Key words Monte Carlo simulation · Radiation treatment planning system · User interface

E. Kunieda (✉) · H.M. Deloar[1] · T. Kawase · A. Kubo
Department of Radiology, Keio University, 35 Shinanomachi, Shinjuku-ku, Tokyo, Japan
Tel. +81-3-3353-1211 (ext. 64444); Fax +81-3-3359-7425
e-mail: kunieda-mi@umin.ac.jp

E. Kunieda · H.M. Deloar · T. Kawase · H. Saitoh · K. Saito
CREST, Japan Science and Technology Agency, Tokyo, Japan

S. Takagi · O. Sato
Safety Engineering and Technology Department, Mitsubishi Research Institute, Tokyo, Japan

K. Sato
Mitsubishi Space Software, Amagasaki, Hyogo, Japan

H. Saitoh
Department of Radiological Sciences, Tokyo Metropolitan University of Health Sciences, Tokyo, Japan

K. Saito
Center for Promotion of Computational Science and Engineering, Japan Atomic Energy Research Institute, Tokai-mura, Japan

G. Sorell
Medical Physics and Bioengineering Department, Christchurch Hospital, Christchurch, New Zealand

Present address:
[1]Medical Physics and Bioengineering Department, Christchurch Hospital, Private Bag 4710, Christchurch, New Zealand

Introduction

BEAMnrcMP Monte Carlo (MC) code[1] based on EGS4[2] is widely recognized as providing accurate calculation of particle transport through the accelerator head. DOSXYZnrc[3] is a general-purpose Monte Carlo EGSnrcMP[4] user code for three-dimensional absorbed dose calculations. The available graphics user interface of BEAMnrc, known as "dosxyz_show"[5] can only display the dose of DOSXYZnrc on the phantom or computed tomography (CT) phantom (egsphant) data in the form

of isodose distributions. A radiotherapy treatment plan (RTP) requires contouring the target structure, including parameters such as gross tumor volume (GTV), clinical target volume (CTV), planning target volume (PTV), and organs at risk (OARs), to evaluate the dose distribution quantitatively in the form of an integral or differential dose-volume histogram (DVH). It is also important to analyze treatment parameters such as dose conformity and dose homogeneity as well as maximum, minimum, and average doses described in a treatment plan as suggested by the International Commission on Radiation Units and Measurements (ICRU) reports 50 and 62.[6,7]

Therefore, the display of the dose from DOSXYZnrc on a dedicated RTP system could provide all of the facilities needed to evaluate an MC dose plan. In this study, we have developed interface software (interface) to display the DOSXYZnrc MC dose on the XiO RTP system. The interface can export three-dimensional MC dose files into the XiO RTP system and is helpful for evaluating MC doses in the form of DVH, dose conformity, dose homogeneity, and so on.

Materials and methods

Interface descriptions

We have developed an interface to read and analyze the MC dose file on the XiO RTP system (version 4.2; CMS, St. Louis, MO, USA). The flow chart of the interface is shown in Fig. 1. The DOSXYZnrc code[3] allows sources such as a monoenergetic diverging or parallel beam, phase-space data generated by a BEAMnrc[1] simulation,

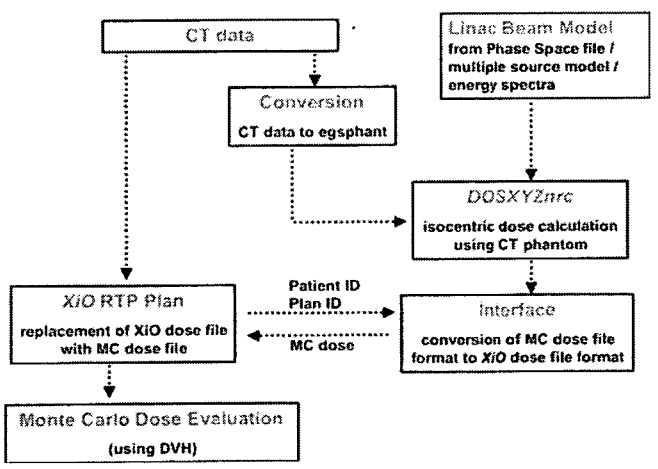

Fig. 1. Flow chart to display the Monte Carlo (*MC*) dose on an XiO radiation treatment planning (*RTP*) system. *CT*, computed tomography

or a model-based beam reconstruction produced by BEAMDP.[3] To calculate the MC dose using CT data, CT values of images need to be converted to physical densities and written into a CT phantom file, which is suffixed *egsphant*.[3] Various sources to model the beam from energy spectra, including phase space files, can be used in DOSXYZnrc. The user may define the incident angles of the phase space beam by changing angles theta and phi.[3] In the polar coordinate system, the polar angle theta has a range of 0°–180°, and the azimuthal angle phi has a range of 0°–360°. In our simulations, we applied different beams around the gross tumor volume (GTV) in the *egsphant* file by changing the angles theta and phi.

The CT data to be used for MC dose calculations needs to be exported to the XiO RTP system to make an arbitrary plan; and later this arbitrary planned dose can be replaced with the MC dose using the interface. The interface is keyboard-interactive and works in two steps: (1) conversion of an MC dose file into XiO dose file format; and (2) export of the MC dose file to the XiO RTP system and replacement of the XiO RTP dose file with the MC dose file.

The conversion procedure requires input of the coordinate of the reference point that appears on the XiO plan and a calibration factor to convert the MC dose per particle to absolute dose. Usually the reference point coordinate is defined at the center of the isocenter slice, and the corresponding coordinate in the *egsphant* file for the MC dose calculation procedure should be the same as in XiO. Variations of that coordinate between XiO and the *egsphant* file may cause a mismatch between the MC dose and the CT structure in the XiO plan; therefore, input of the coordinate from the XiO reference point adjusts all of the coordinates of the MC dose file to fit with the CT coordinate system in the XiO plan. This is extremely important for exact spatial display of the MC dose on the CT structure of the XiO plan.

During the procedure for replacing the XiO dose file with the MC dose file, the patient identification (ID) and plan ID are needed from the XiO plan. Upon execution of the interface with the patient and plan IDs, the XiO dose file is replaced with the MC dose file, and the XiO dose file is converted to a backup file.

Interface evaluations

Evaluations of the interface were performed with three data sets, which is considered to be enough for evaluating the system. MC doses are calculated based on the three data sets: CT data from a thorax phantom; human CT data from a patient with a lung tumor; and a uniform phantom. The thorax phantom consisted of three densi-

ties: The density of the lung region was 0.3 g/cc; the density of the tumor (GTV) and other soft tissue-equivalent material was 1.0 g/cc; and the density of the spine was 1.3 g/cc. The GTV was 2 cm ϕ and was situated in the center of the right lung. CT scans of the thorax phantom were performed to obtain CT images. Patient-specific CT images of a lung tumor and finally a cylindrical uniform phantom of water-equivalent density were also used to evaluate the interface by analyzing the MC doses on the XiO RTP system. In all cases (thorax phantom, human lung, and uniform phantom), the thickness of the CT slices was 2 mm, and the matrix size of each slice was 512 × 512 pixels. All CT numbers in CT images in this study were converted to *egsphant* data using the corresponding electron density data. The matrix size of *egs4phant* data was reduced to 256 × 256 pixels; these data were used in the Monte Carlo dose calculation system.

In our previous work we modeled the linac systems for 6-, 10-, and 18-MV photons,[8] and the particle data were stored in a phase space file.[1] The full-phase space files were applied to calculate MC doses using the thorax phantom for 6-, 10-, and 18-MV energies. Beams of 3 × 3 cm were employed from four directions around the center of the GTV of the thorax phantom.

Exact spatial positioning of the MC dose on CT structures in the form of isodose distributions in the XiO plan is important, and the position was verified with previous work with MC doses calculated for patient CT images of a lung tumor using 200-, 300-, and 500-kVp X-ray energies; those energies were modeled previously to evaluate a kilo-voltage 3DCRT system.[9] Three noncoplanar converging arcs around the center of the GTV were employed to calculate the MC dose for human lung with 200-, 300-, and 500-kVp X-ray energy. A 3 × 3 cm beam size was used in the dose calculation procedure and for three couch angles, 0° and ± 25°, the gantry rotation around the target was 200° both for the thorax phantom (160°–360°) and human lung (190°–30°).

Further evaluation of the interface was performed by comparing the MC and XiO dose distributions calculated for a uniform phantom. The XiO dose calculations were performed using a superposition algorithm.[10,11] A coplanar arc around the center of the uniform phantom was employed to calculate dose distributions for linac energies of 6, 10, and 18 MV and a beam size of 4 × 4 cm.

All MC dose calculations were performed for 300 million photon events. The global electron and photon cutoff energies in kilovoltage dose calculations were 0.5 and 0.001 MeV, and the corresponding values in the MV dose calculations were 0.7 and 0.001 MeV, respectively.

Results

Using the interface, all MC doses calculated with DOSXYZnrc that were loaded into the XiO RTP system for quantitative evaluation were displayed on the CT structure of the XiO plan in the form of isodose distributions. An example of a display of MC dose on the XiO RTP system for 6-MV photon energy is shown in Fig. 2, in which the transverse, coronal, and sagittal views of the images are displayed with isodose lines and DVHs. A comparative study of MC DVHs for 6, 10, and 18 MV of energy extracted from the XiO plan is shown in Fig. 3; for each energy the differential DVHs were extracted from the XiO plan and then for comparison the cumulative DVHs in Fig. 3 were reconstructed. As the MC dose calculations and the dose visualizations on the RTP system are in two different environments, it is important to ensure the spatial positioning of the MC dose distributions on the CT structure of the XiO plan. These verifications were done with the MC doses calculated for patient CT images of a lung tumor using 200-, 300-, and 500-kVp X-ray energy; and these dose distributions were shown on transverse and coronal planes taken through the isocenter (Fig. 4).

Low-energy X-rays are sensitive to high-Z materials, and therefore the high density of the rib bones caused an elevation in absorbed dose due to photoelectron absorption. Nevertheless, absorption of the dose by bone from kVp X-rays ensured the spatial positioning of the MC dose in the CT structure of the XiO plan. The range of the apparent dose to the ribs was 80%–90% for 200 kVp, 40%–60% for 300 kVp, and 20%–40% for 500 kVp; and the maximum dose was normalized to 100% at the center of the GTV. The DVHs of the GTV delineated on human lung tumor for 200, 300, and 500 kVp are shown in Fig. 5. The DVH of 500 kVp is better than the histograms of the other energies. To analyze DVHs on the XiO RTP system, the doses in all cases were normalized with respect to the dose at the center of the GTV.

The MC and XiO dose calculations were performed for linac energies of 6, 10, and 18 MV using a uniform cylindrical phantom. Their profiles through the isocenter were compared (results not shown), and good agreement was observed.

Discussion

The Monte Carlo method has been demonstrated to be an accurate method for dose calculations in radiotherapy.[1,12–15] The BEAMnrcMP code based on EGS4[2] is extensively used for modeling radiotherapy sources, and